Catalysis Today 143 (2009) 203–210

Contents lists available at ScienceDirect

Catalysis Today

journal homepage: www.elsevier.com/locate/cattod

Comparison of the photocatalytic degradation of 2-propanol in gas–solid and liquid–solid systems by using TiO_2–$LnPc_2$ hybrid powders

G. Marcì [a], E. García-López [a,*], G. Mele [b], L. Palmisano [a], G. Dyrda [c], R. Słota [c]

[a] "Schiavello-Grillone" Photocatalysis Group, Dipartimento di Ingegneria Chimica dei Processi e dei Materiali, Università degli studi di Palermo, Viale delle Scienze, 90128 Palermo, Italy
[b] Dipartimento di Ingegneria dell'Innovazione, Università del Salento, Via Arnesano, 73100 Lecce, Italy
[c] Faculty of Chemistry Opole University, Oleska 48, 45-095 Opole, Poland

ARTICLE INFO

Article history:
Available online 7 February 2009

Keywords:
Lanthanide bis-phthalocyanines
2-Propanol
Heterogeneous photocatalysis
TiO_2

ABSTRACT

Photocatalytic degradation of 2-propanol was carried out as a probe reaction both in gas–solid and in liquid–solid systems in the presence of TiO_2 both bare and impregnated with lanthanide (Sm, Gd, Ho) bis-phthalocyanines ($LnPc_2$) used as sensitizers. Continuous and batch photo-reactors, irradiated with an equal flux of photons, were used in gas–solid and in liquid–solid systems, respectively. Propanone and acetaldehyde were the main intermediates found in both systems during 2-propanol oxidation, whereas carbon dioxide and water were the final oxidation products exclusively in the gas–solid regime. The photocatalysts exhibited significantly higher activity in the liquid–solid system than in the gas–solid one. Samples impregnated with the sensitizers were apparently more photoactive than bare TiO_2. The highest photoactivity was shown by the 1.85 $HoPc_2$–TiO_2 sample.

1. Introduction

Macrocyclic molecules such as phthalocyanine derivatives (MPc, where M = 2H or coordinated metal, Pc = $C_{32}H_{16}N_8$), firstly developed as industrial pigments, have been receiving an increasing interest for their technological applications including solar cells [1], homogeneous and/or heterogeneous catalysts [2–6], modified electrodes [7–8], optical filters [9], gas sensors [10] and photodynamic therapy [11]. There is a close relationship between phthalocyanines and porphyrins, evidently manifested by similar aromatic π-electronic cores, which determine the chemistry of these compounds (Fig. 1). The central metal template stabilizes the macrocyclic molecular set-up, in principle regardless of the complex's structure. Hence, phthalocyanine systems containing one, two or three Pc ligands may be synthesized, depending on the chemical properties of the coordinated metal. The molecular stability and physicochemical properties of metallophthalocyanines, especially their spectrochemical features as well as their photocatalytic behaviour, depend on the character of the interactions between the metal and the Pc ligand.

Rare earth metal diphthalocyanines ($LnPc_2$, where Ln = Ce. . .Lu), first synthesized in the 1960s [12], revealed a range of unique features not shown by the mono-phthalocyanines, MPcs. The more sophisticated molecular structure (Fig. 1) and hence the different electronic properties, reflected in their variable, medium-related UV–vis spectra (Fig. 2) make the $LnPc_2$s particularly interesting for applications involving specific photochemical activity. In addition, these peculiar double-decker systems proved very stable under illumination by UV and visible light, evidently more than the MPcs [13]. High photostability, resulting from the existence of a relative flexible system of conjugated π-bonds in the coupled macrocycles of a $LnPc_2$ unit, was also demonstrated in air-saturated solvents [14]. Such properties may be crucial to the catalytic behaviour of lanthanide bis-phthalocyanines. A wide commercial application of phthalocyanines has been limited because of their low solubility in most of organic solvents.

Titanium dioxide, an inexpensive, non-toxic and biocompatible material, is one of the most important and widely investigated photocatalysts because of its application in decomposition of various environmental pollutants in both gaseous and liquid systems [15–17]. Development of a new class of TiO_2-based photocatalysts impregnated with sensitizers like the $LnPc_2$s would be of great significance in terms of thermal and photo-stability. Both parameters are important to gain significant advantages in a photocatalytic process and may considerably improve the yield of photosensitized reactions. Composite TiO_2–$LnPc_2$ photocatalysts proved effective in degradation of a common water pollutant, 4-nitrophenol, as reported in a previous paper [18].

2-Propanol (2-PrOH) was chosen as a model reactant because this molecule is a major contaminant in indoor air and air streams

* Corresponding author.
E-mail address: garcia@dicpm.unipa.it (E. García-López).

0920-5861/$ – see front matter © 2009 Elsevier B.V. All rights reserved.
doi:10.1016/j.cattod.2008.12.029

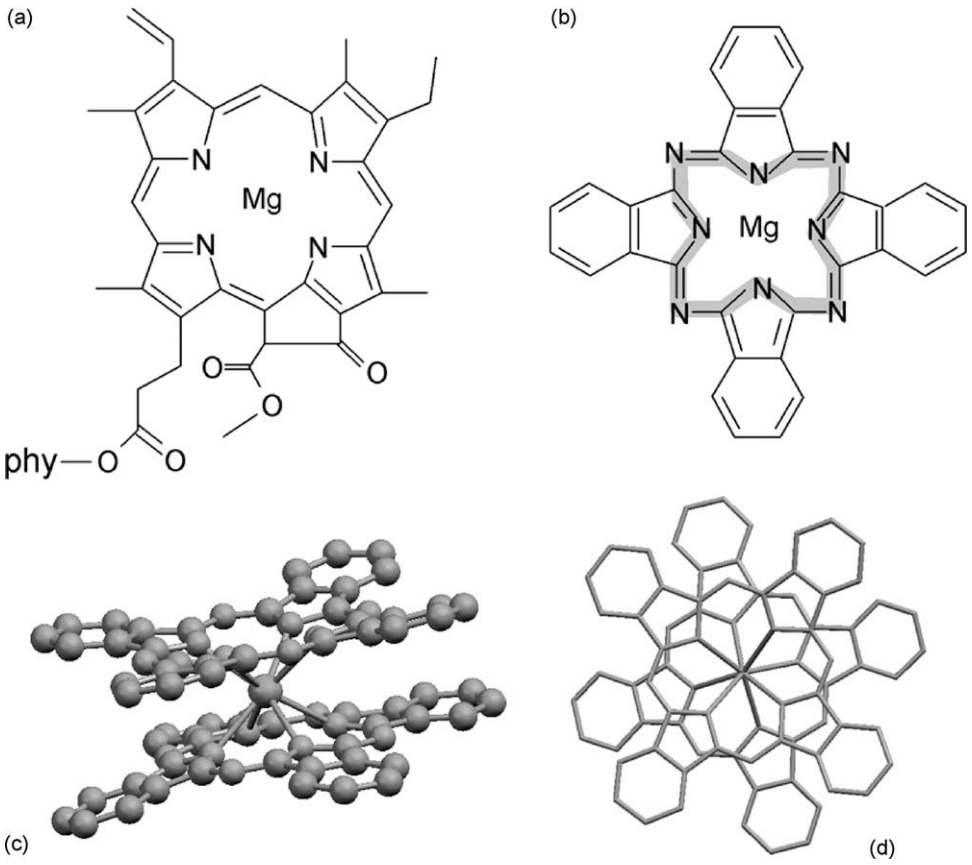

Fig. 1. Molecular structure of porphyrin analogues: (A) chlorophyll *a* (*phy*–phytol chain, $C_{20}H_{39}$); (B) MgPc (π-electronic core highlighted); (C) $HoPc_2$, general representation; (D) top view of the coupled phthalocyanine macrocycles in $HoPc_2$.

[19]. Its adsorption and decomposition on TiO_2 surfaces has been studied both in gas–solid [20–22] and in liquid–solid systems [23–25]. In both cases, the decomposition can proceed according to two pathways by either dehydrogenation or dehydration, giving rise to propanone or propene, respectively. The presence of propene has also been justified by considering the hydroxylation of the transient product 2-propoxide during 2-PrOH oxidation [21]. The selectivity to these intermediate products strongly depends on the experimental conditions and particularly on the acid–base properties of the solid photocatalyst. In fact, it is suggested that dehydration of 2-PrOH into propene results from the catalyst acidic character, whereas its dehydrogenation to propanone is due to its basicity [26,27]. It is worth to note, moreover, that 2-PrOH dehydrogenation is also favoured in a system which has displayed oxidizing properties. Propanone was almost always reported to be the main intermediate during the catalytic oxidation of 2-PrOH, to produce ultimately CO_2. Isopropyl ether was also observed at a trace level as an intermediate during 2-PrOH oxidation [28] and the use of TiO_2 samples modified by incorporating sulfuric acid or ammonium sulfate led to a high selectivity towards isopropyl ether or propene, respectively [29]. More recently nanoparticles of Pt loaded on the TiO_2 surface prepared by microemulsion techniques increased significantly the degradation rate of 2-PrOH [30].

In this work, commercial TiO_2-anatase samples, impregnated with lanthanide bis-phthalocyanine sensitizers, including the Sm, Gd and/or Ho elements, were used for the photo-oxidation of 2-PrOH carried out both in gas–solid and in liquid–solid systems. This investigation allowed to estimate the influence of the reaction medium upon the system's photoactivity. Moreover some intermediates and final products were identified.

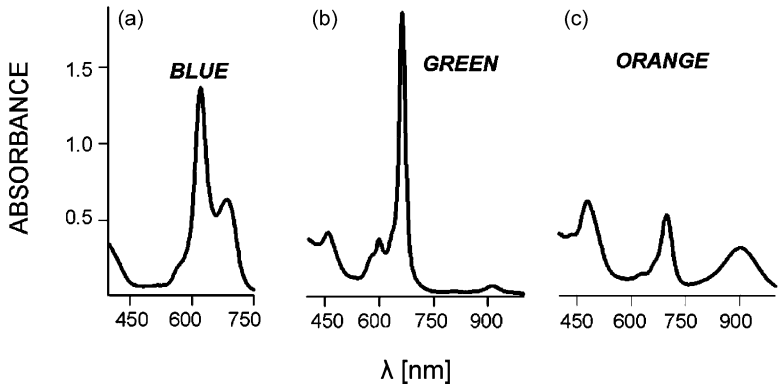

Fig. 2. Basic types of electronic absorption spectra featuring diverse colored forms of $HoPc_2$: (A) *blue* form in DMF; (B) *green* form in CH_2Cl_2; (C) *orange* form generated in CH_2Cl_2 by UV irradiation (λ = 366 nm).

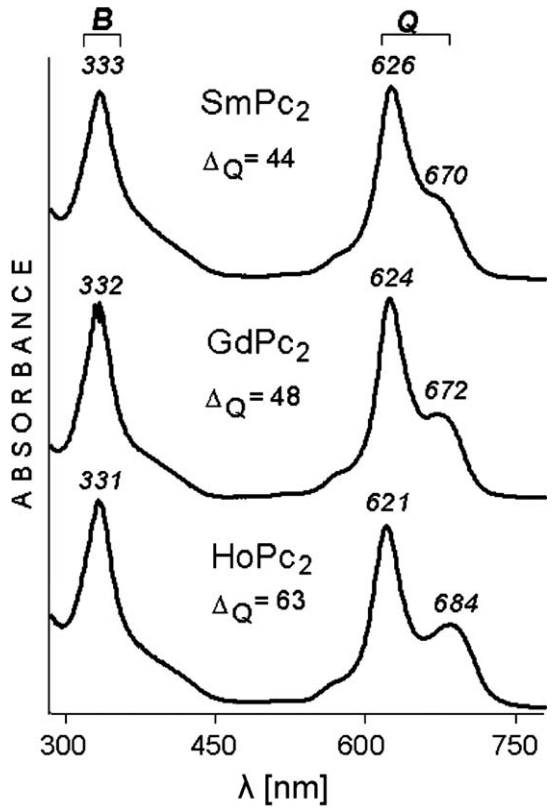

Fig. 3. Absorption spectra of the *blue* forms of Sm, Gd and Ho bis-phthtalocyanines (in DMF) featuring the *Q*-band splitting (Δ_Q, nm).

2. Experimental

2.1. Preparation and characterization of the photocatalysts

The $LnPc_2$ complexes of Sm, Gd and Ho were synthesized and purified in our laboratory (ICh Opole) according to the method applied by Kirin et al. [12] under modified reaction conditions as described elsewhere [17]. This procedure has allowed to obtain the blue form-$LnPc_2$ compounds characterized by the absorption spectra shown in Fig. 3. Very strong absorption bands at $\lambda \approx 330$ nm (B) and 620–630 nm (*Q*, split) with molar absorptivities $\varepsilon > 10^5$, accompanied by a satellite-band at 670–690 nm with ca. three times less intensity, do distinguish the $LnPc_2$ complexes from the other members of the phthalocyanine family. Typical MPcs exhibit only one strong absorption band (Q) in the range of ca. 660–700 nm (metal and solvent-related) revealing no splitting, whereas the intensity of the B-band ($\lambda \approx 340$ nm) is approximately two times lower [31]. The *Q*-band splitting observed in $LnPc_2$ reflects the interaction between the lanthanide atom and the π-electronic systems of the individual macrocycles and its extent depends on the hosted Ln element and the solvent used.

2.2. Photoreactivity experiments in the gas–solid system

The photoreactor operating in the gas–solid system was a continuous pyrex photoreactor of cylindrical shape (diameter: 58 mm; height: 100 mm). A porous glass septum on the bottom of the cylinder allowed to sustain the fixed bed of the solid and to distribute the inlet gaseous mixture. The height of the fixed bed was ca. 1 mm. Reactivity runs were carried out with 1 g of the photocatalyst. Bare TiO_2 used in these experiments was provided by Tioxide Huntsman (100% anatase, specific surface area 8 m^2 g). Lanthanide bis-phthalocyaninato complexes of Sm, Gd, and Ho supported on the same commercial polycrystalline TiO_2 were applied as photosensitizers. Only the most active loaded samples, which primarily proved effective in photocatalytic oxidation of 4-nitrophenol in a liquid–solid regime [18], containing 1.38 μmol, 1.85 μmol and 3.30 μmol of the Sm, Gd, and Ho sensitizer, respectively per 1 g of TiO_2 were tested.

The gas feeding the photoreactor was composed of oxygen, 2-PrOH and water vapor. 2-PrOH and water were introduced in the oxygen stream by means of a home made infusion pump. Initial concentrations of 2-Pr–OH in the gas phase were 2×10^{-5} M and 8×10^{-5} M (i.e. 915 ppm and 3660 ppm, expressed in mg of 2-Pr–OH per 1 kg of oxygen in the gas phase). The concentration of water was 3.4×10^{-4} M (4680 ppm) and during some selected runs it was not fed into the system. Preliminary tests were performed to determine the suitable flow rate conditions to avoid mass transport limitations during the photoreaction. Consequently the flow rate at which the runs were carried out was set at 0.5 cm^3 s^{-1}. The irradiation started only after the steady state conditions were achieved, i.e. after about 2 h of gas feeding. The reactor was vertically fixed inside of a SOLARBOX apparatus (CO.FO.ME.GRA.) equipped with a 1500 W Xe lamp and it was illuminated from the top. A water filter was located between the lamp and the photoreactor to cut-off the infrared radiation and to maintain the temperature inside the reactor at ca. 300 K. The irradiance onto the photoreactor was measured by using the radiometer UVX Digital and it was equal to 1.5 mW cm^{-2}, corresponding to $\Phi_i = 1.19 \times 10^{-7}$ einstein s^{-1}. The runs lasted ca. 4.5 h. Samples of the reacting fluid were analysed by withdrawing 200 μL of gas from the outlet of the photoreactor by means of a gas-tight syringe at fixed intervals of time. Concentrations of the substrate and intermediates were measured by a GC-17A Shimadzu gas chromatograph equipped with a HP-1 column and a FID, whereas carbon dioxide was analyzed by a Carboxen column in an HP6890 gas chromatograph equipped with a TCD.

2.3. Photoreactivity experiments in the liquid–solid system

In experiments carried out in the liquid–solid regime a 75 mL sealed batch photoreactor with irradiated surface of 25.13 cm^2 was used. Pure oxygen was bubbled into the suspensions for ca. 0.5 h prior to switching the lamp on. The photoreactor was irradiated by means of the SOLARBOX apparatus and an IR filter was also used in this case. The light flux impinging onto the photoreactor was the same as applied in the gas–solid system ($\Phi_i = 1.19 \times 10^{-7}$ einstein s^{-1}). The initial concentrations of 2-PrOH in aqueous solutions were 15×10^{-3} M and 61×10^{-3} M (i.e. 915 ppm and 3660 ppm, expressed in mg per 1 L of solution) at natural pH (ca. 6.5) and the amount of catalyst used in each experiment was 1 g L^{-1}. The photoreactivity runs lasted 5 h. Samples of the reacting suspension were withdrawn from the reactor at fixed times and the catalysts were separated from the solution by filtration through 0.45 μm cellulose acetate membranes (HA, Millipore). The quantitative determination of the substrate and intermediate products was performed by injecting 1 μL of the liquid sample into the gas chromatograph applying the same method as described above. The evolution of CO_2 during the photoreaction was assayed by means of a Carboxen column in an HP6890 gas chromatograph equipped with a TCD by withdrawing a gas sample in equilibrium with the reacting suspension by means of a gas-tight syringe.

3. Results and discussion

3.1. Photoreactivity experiments

For both the gas–solid and liquid–solid systems, blank reactivity tests were performed under the same experimental

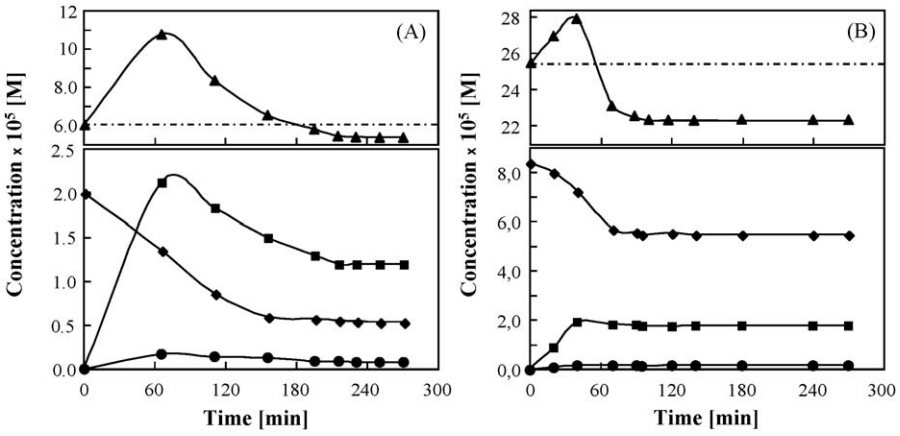

Fig. 4. Evolution of 2-PrOH (◆), propanone (■), and acetaldehyde (●) concentrations at the outlet of the continuous photoreactor and total carbon amount present in 2-PrOH, propanone and acetaldehyde (▲) vs. irradiation time for reaction in the gas–solid system in the presence of bare TiO_2. Initial 2-PrOH concentrations: (A) 915 ppm (2×10^{-5} M); (B) 3660 ppm (8×10^{-5} M). Dotted line represents the total carbon amount fed to the reactor.

conditions used in the photo-reactivity experiments but in the absence of catalyst, oxygen or light. Since no reactivity was observed in all these cases, it can be concluded that O_2, catalyst and radiation must be simultaneously used to successfully perform the photo-oxidation of 2-PrOH.

A preliminary investigation was carried out in order to establish if the supported sensitizers were photostable, i.e. if some decomposition or chemical modification took place under the same conditions used during the photocatalytic experiments. Total organic carbon (TOC) determinations in the absence of substrate indicated no release of organic degradation compounds even after long irradiation times (5–7 h).

3.1.1. Gas–solid system: fixed bed continuous photoreactor

The photoreactivity runs started when the system achieved the steady state conditions under dark, i.e. when the outlet concentration of 2-PrOH was higher than 95% of the inlet value.

Fig. 4 reports the values of the outlet 2-PrOH concentration versus irradiation time for two runs carried out by using bare TiO_2 as the photocatalyst at two initial 2-PrOH concentrations and in the presence of water vapor. Fig. 5 reports the evolution of the substrate for runs carried out under the same conditions as in Fig. 4 by using 1.85 $HoPc_2$–TiO_2 as the photocatalyst. Figs. 4 and 5 show also the evolution of propanone, acetaldehyde and the total carbon amount calculated by adding the carbon content of 2-PrOH, propanone and acetaldehyde analyzed.

A decrease in concentration of 2-PrOH is evident in Figs. 4 and 5, even if it does not completely disappear. A simultaneous increase in propanone and acetaldehyde concentrations is also observed. The amount of propanone is always higher than that of acetaldehyde that increases more slowly than propanone, but both compounds reach an almost constant value after 2–2.5 h of irradiation.

The initial increase of the total carbon amount, just after switching on the lamp, can be attributed to a fast degradation of some quantity of the substrate adsorbed during the stabilization period under dark. Once the steady state conditions were fulfilled, the mass balance of carbon was not completely satisfied. Perusal of Figs. 4 and 5 reveals that 2-PrOH was never quantitatively transformed into propanone and acetaldehyde. In fact, carbon dioxide was simultaneously generated and the apparent loss in carbon mass (ca. 10–20%) at steady state conditions refers (within the experimental error limits) to the amount of CO_2 analyzed in the gas phase. Moreover, traces of isopropyl ether and propene were also found among the gaseous products.

The comparison of Figs. 4 and 5 does not show significant differences between the behaviour of bare TiO_2 and 1.85 $HoPc_2$–TiO_2 samples, as far as the type and relative amounts of intermediates are concerned.

Table 1 reports the 2-PrOH disappearance rate ($r_{2\text{-PrOH}}$), its % conversion, yield of propanone and acetaldehyde and the quantum efficiency (η). The 2-PrOH disappearance rate was calculated by

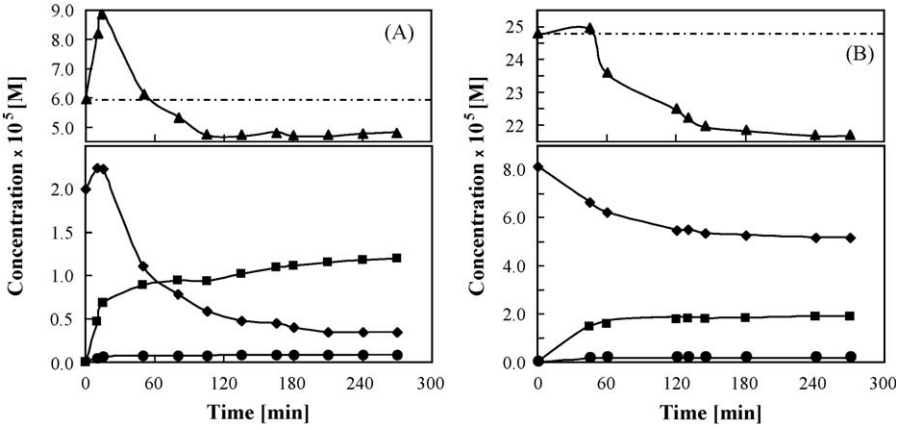

Fig. 5. Evolution of 2-PrOH (◆), propanone (■), and acetaldehyde (●) concentrations at the outlet of the continuous photoreactor and total carbon amount present in 2-PrOH, propanone and acetaldehyde (▲) vs. irradiation time for reaction in the gas–solid system in the presence of 1.85 $HoPc_2$–TiO_2. Initial 2-PrOH concentrations: (A) 915 ppm (2×10^{-5} M); (B) 3660 ppm (8×10^{-5} M). Dotted line represents the total carbon amount fed to the reactor.

Table 1
Reactivity results for 2-PrOH disappearance determined in the gas–solid system. The values reported in the table are the average of three measurements.

	TiO_2	1.38 $SmPc_2$–TiO_2	1.85 $HoPc_2$–TiO_2	3.30 $GdPc_2$–TiO_2
2-PrOH initial concentration = 915 ppm				
$r_{2\text{-PrOH}}$ (mol s^{-1})	7.32×10^{-9}	7.28×10^{-9}	8.25×10^{-9}	7.75×10^{-9}
Conversion 2-PrOH (%)	73	73	83	75
Yield propanone (%)	83	73	70	80
Yield acetaldehyde (%)	6	6	5	6
η (%)	6.1	6.1	7.0	6.5
2-PrOH initial concentration = 3660 ppm				
$r_{2\text{-PrOH}}$ (mol s^{-1})	1.45×10^{-8}	1.48×10^{-8}	1.48×10^{-8}	1.48×10^{-8}
Conversion 2-PrOH (%)	34	36	36	33
Yield propanone (%)	62	54	66	70
Yield acetaldehyde (%)	6	4	6	7
η (%)	12.2	12.4	12.4	12.4

applying the following mass balance equation to the whole photoreactor:

$$r_{2\text{-PrOH}} = W(C^{o}_{2\text{-PrOH}} - C_{2\text{-PrOH}}) \quad (1)$$

in which W is the volumetric gas flow rate, whereas $C^{o}_{2\text{-PrOH}}$ and $C_{2\text{-PrOH}}$ are the inlet and outlet molar concentrations of 2-PrOH, respectively. The quantum efficiency (η) was calculated by dividing the reaction rate by Φ_i (number of moles of photons impinging on the photoreactor per second, in this work $\Phi_i = 1.19 \times 10^{-7}$ einstein s^{-1}).

The figures presented in Table 1 show that the reaction rate for each photocatalyst was almost doubled by raising the initial concentration of the substrate from 915 ppm to 3660 ppm. This fact could be explained by assuming that only a part of the active sites was covered by 2-PrOH at the lower initial concentration.

The runs performed at 915 ppm of 2-PrOH by using the hybrid TiO_2–$LnPc_2$ catalysts impregnated with Ho and Gd complexes were slightly faster than those observed when bare TiO_2 was used. On the contrary, when the initial substrate concentration was 3660 ppm the reaction rates measured by using the various photocatalysts were similar. The higher initial concentration of 2-PrOH seems to have a leveling effect on the reaction rate, indicating a saturation of the active sites. This hypothesis is supported by the fact that when the initial concentration of 2-PrOH raised four times the reaction rate increased only twice. This fact justifies also that the lower the initial concentration of 2-PrOH, the higher the conversion.

The above results suggest that the optimum value of initial 2-PrOH concentration must lie between 915 ppm and 3660 ppm.

At higher initial concentration of 2-PrOH, propanone yield slightly decreased, indicating a probable competition between 2-PrOH and propanone for the surface active sites, as reported elsewhere [22]. However, the yield in acetaldehyde practically did not change at the higher initial concentration of the substrate.

In order to study the influence of water vapor on the photoreactivity, some experiments were carried out in its absence. Under the applied experimental conditions it can be concluded that the presence of water vapor (3.4×10^{-4} M) does not influence the performance of the solid photocatalyts. This finding may be explained by considering the formation of water as a reaction product [19–22,26]. It is reported in the literature that the presence of water is essential to displace propanone from the surface [21]. The discussed results indicate that the quantity of water produced during the reaction is sufficient to allow the restoration of the active sites. Moreover, no deactivation of the catalysts was noticed either in the presence or in the absence of water. The behaviour of 2-PrOH contrasts with that observed with some aromatic molecules, e.g. toluene [32] for which deactivation occurred also in the presence of water vapor in the gas–solid system using TiO_2 Degussa P25, due to the strong interaction of benzoate species produced onto the surface active sites.

3.1.2. Liquid–solid system: batch photoreactor

Degradation of 2-PrOH in the liquid–solid system, as follows from Fig. 6, displays a zero order kinetics regardless of the initial concentration of 2-PrOH and the applied catalyst. The reaction rates, calculated from the best linear fits of experimental results, as well as the quantum efficiency have been collected in Table 2.

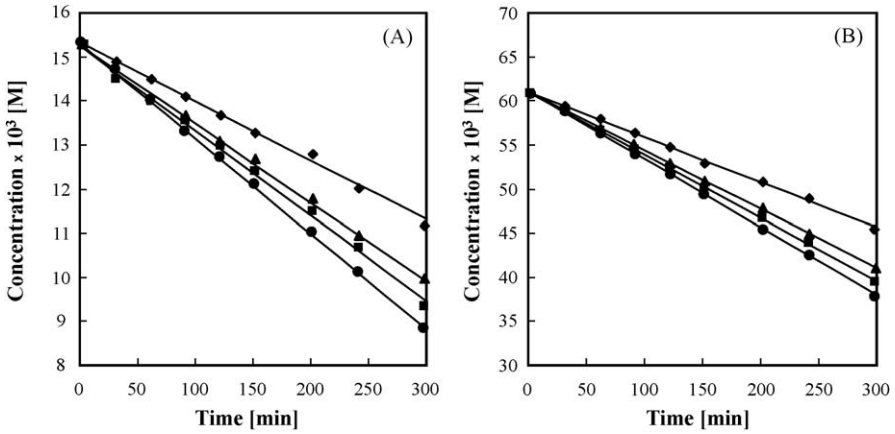

Fig. 6. Evolution of 2-PrOH concentration vs. irradiation time for reaction in the liquid–solid system. Initial 2-PrOH concentrations: (A) 915 ppm (15×10^{-3} M); (B) 3660 ppm (61×10^{-3} M). Photocatalysts: TiO_2 (◆), 3.30 $GdPc_2$–TiO_2 (■), 1.38 $SmPc_2$–TiO_2 (▲), and 1.85 $HoPc_2$–TiO_2 (●).

Table 2
Reactivity results for 2-PrOH disappearance determined in the liquid–solid system. The values reported in the table are the average of three measurements.

	TiO_2	1.38 $SmPc_2$–TiO_2	1.85 $HoPc_2$–TiO_2	3.30 $GdPc_2$–TiO_2
2-PrOH initial concentration = 915 ppm				
$r_{2\text{-PrOH}}$ (mol s^{-1})	1.67×10^{-8}	2.20×10^{-8}	2.70×10^{-8}	2.40×10^{-8}
η (%)	14.0	18.5	22.7	20.2
2-PrOH initial concentration = 3660 ppm				
$r_{2\text{-PrOH}}$ (mol s^{-1})	6.40×10^{-8}	8.30×10^{-8}	9.60×10^{-8}	8.90×10^{-8}
η (%)	53.8	69.8	80.7	74.8

The value of $r_{2\text{-PrOH}}$ increased four times by raising four times the initial concentration of 2-PrOH (from 915 ppm to 3360 ppm), unlike in the gas–solid system. The linear increase of reaction rate with the initial concentration of the substrate could be explained by assuming that the photocatalytic oxidation could have occurred not only within the surface-adsorbed layer involving both the OH radicals and the holes directly trapped by the substrate, but also in the homogeneous phase. In the latter, both interfacial OH radical and singlet oxygen, which may be generated by photosensitized phthalocyanines [33] could play a significant role. Particularly, OH radical species can diffuse several angstroms from the surface to the solution [34] before being trapped by 2-PrOH molecules in the fluid phase [35].

The runs carried out in the presence of TiO_2–$LnPc_2$ photocatalysts were always faster than when bare TiO_2 was used. Again, the best performance was revealed by the 1.85 $HoPc_2$–TiO_2 sample, featuring a ca. 1.5 times faster photoreaction with respect to the bare TiO_2, both at 915 ppm and 3660 ppm.

The determined quantum efficiency (η) was greater than the values reported elsewhere for other probe molecules [6] and it was found to increase linearly by raising the initial concentration of 2-PrOH. Such high η values can be explained by hypothesizing the occurrence of oxidative reactions not only on the TiO_2 surface but also in the liquid phase. Moreover, a beneficial effect of water to regenerate the surface sites cannot be neglected. Hence, the presence of lanthanide bis-phthalocyanines had a beneficial effect on the activity of the photocatalysts in both reaction systems only when the initial concentration of 2-PrOH was 915 ppm. These results are in agreement with those obtained with 4-nitrophenol by using the same photocatalysts [18]. Also in this case, the 1.85 $HoPc_2$–TiO_2 hybrid demonstrated the highest photoactivity. As reported before, photo-excitation of TiO_2 is essential to promote the photoreaction in the presence of phthalocyanine and/or porphyrin sensitizers adsorbed onto the surface of TiO_2 solids [6]. In other words, the results obtained so far confirm the existence of a cooperative mechanism involving photo-excitation of the semiconductor, which needs photons from the range of λ = 300–400 nm, as well as the sensitizer, which may occur also under visible light. A beneficial effect of the sensitizer is noticeable only in some cases because it depends on the kind and on the amount of the species loaded onto the TiO_2 surface, i.e. it is related to the availability of the active sites. In fact, when the initial substrate concentration was 3660 ppm, only in the liquid–solid system the reaction rate in the presence of the sensitized samples was still higher.

In Fig. 7 photodegradation of 2-PrOH is shown for a selected run in the presence of 1.85 $HoPc_2$–TiO_2 in the liquid–solid system. The reaction yielded simultaneously propanone and acetaldehyde and their concentrations continuously increased during the irradiation; however, the quantity of the latter appeared much lower. The mass balance of total carbon was maintained in this case and, in contrast to the results obtained in the gas–solid system, no CO_2 was found among the products. This fact indicates that the

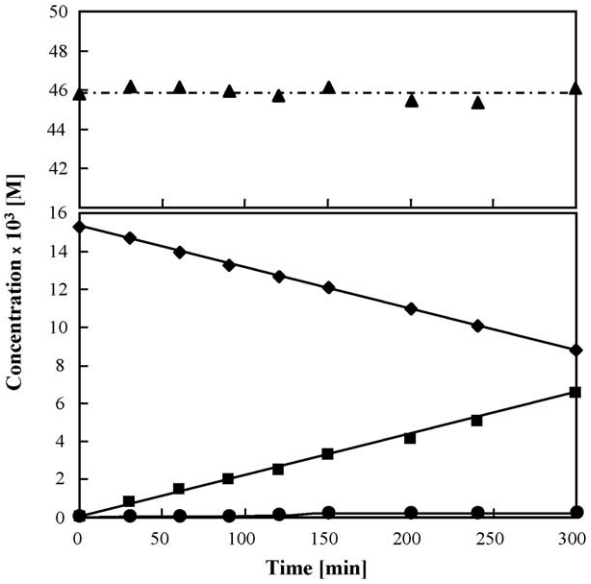

Fig. 7. Evolution of 2-PrOH (◆), propanone (■), and acetaldehyde (●) concentrations and total carbon amount (▲) vs. irradiation time for reaction in the liquid–solid system in the presence of the 1.85 $HoPc_2$–TiO_2 photocatalyst at the initial 2-PrOH concentration of 915 ppm (15×10^{-3} M).

formation of CO_2 is due to the ultimate oxidation of propanone and acetaldehyde. Interestingly, the reaction rate of 2-PrOH disappearance (2.7×10^{-8} mol s^{-1}) is equal to the sum of the appearance rates of propanone (2.5×10^{-8} mol s^{-1}) and acetaldehyde (1.4×10^{-9} mol s^{-1}), within the experimental error. Thus, it has been proved that decay of the organic substrate occurs via two irreversible parallel oxidation routes resulting in propanone and acetaldehyde (see Section 3.2) production.

Reaction rates reported in Tables 1 and 2 appear higher in the liquid with respect to the gas phase, about twofold and/or 5–6 times at the initial concentration of the substrate of 915 ppm and 3660 ppm, respectively. It is clear then, that the liquid–solid system favours the degradation of the substrate and that the reaction is even more favoured the higher the concentration of the substrate is.

The absence of CO_2 among the products obtained in the liquid–solid regime could be justified by the occurrence of a homogeneous reaction. As reported elsewhere, oxidation reactions in the homogeneous phase do not easily achieve complete mineralization of organic molecules [32].

3.2. Mechanistic aspects

The photo-oxidation runs indicated that 2-PrOH degradation occurred via the formation of various intermediates and no significant difference was found between the gas–solid and the liquid–solid systems from a qualitative point of view. It seems that the interfaces do not play a significant role in the reaction mechanism, unlike in experiments using other substrates, e.g. toluene [36] and acetonitrile [37,38] for which different intermediate products were observed depending upon the medium (gas or aqueous phase). As mentioned before, the main intermediates derived from 2-PrOH photo-oxidation in both systems were propanone and acetaldehyde. The same compounds were observed by Bickley et al. [20] in photocatalytic oxidation of isopropanol by TiO_2 in a gas–solid regime. There is a general agreement in the literature that the main products of 2-PrOH photocatalytic oxidation in a gas–solid system are propanone, CO_2 and H_2O, with selectivity versus propanone or CO_2 depending strongly on the experimental conditions [20–26]. Moreover, isopropyl ether

[29] or propene [21] were also revealed. FTIR spectroscopy allowed to observe, besides propanone, also propene [20], mesityl oxide [39] and ethanoic acid [20,40] adsorbed on the catalyst surface. Some species can strongly interact at the surface thus blocking the active sites [20]. In a liquid–solid regime, propanone was reported as the main intermediate [23–25].

It is generally accepted that •OH radicals generated on the surface of the photocatalyst as shown in reactions (2)–(5), act as the primary oxidant species. The hydroxyl radicals are produced in the following reactions:

$$TiO_2 + h\nu \rightarrow TiO_2(e^-_{cb}, h^+_{\nu b}) \quad (2)$$

$$O_{2(ads)} + e^- \rightarrow O^-_{2(ads)} \quad (3)$$

$$OH^-_{(surf)} + h^+_{\nu b} \rightarrow {}^\bullet OH_{(surf)} \quad (4)$$

$$H_2O_{(ads)} + h^+_{\nu b} \rightarrow {}^\bullet OH_{(surf)} + H^+ \quad (5)$$

The reaction between •OH radicals and 2-PrOH gives rise to the formation of propanone and acetaldehyde. Ohko et al. [41] report that the generated •OH radical reacts with 2-PrOH, abstracting a hydrogen atom to form a radical; the role of 2-PrOH as a hole trap, however, cannot be excluded [42], and consequently the disappearance of 2-PrOH could involve two parallel pathways represented by the following reactions:

$$(CH_3)_2CHOH + {}^\bullet OH \rightarrow (CH_3)_2C^\bullet OH + H_2O \quad (6)$$

$$(CH_3)_2CHOH + h^+ \rightarrow (CH_3)_2C^\bullet OH + H^+ \quad (7)$$

$(CH_3)_2C^\bullet OH$ radical may form propanone through different reaction pathways [41]:

$$(CH_3)_2C^\bullet OH + {}^\bullet OH \rightarrow (CH_3)_2CO + H_2O \quad (8)$$

or

$$(CH_3)_2C^\bullet OH + h^+ \rightarrow (CH_3)_2CO + H^+ \quad (9)$$

Analogously, the formation of another radical, obtained according to reactions (10) and/or (11) that can evolve into acetaldehyde and methanol (12), could be hypothesized.

$$(CH_3)_2CHOH + {}^\bullet OH \rightarrow (CH_3)_2CHO^\bullet + H_2O \quad (10)$$

$$(CH_3)_2CHOH + h^+ \rightarrow (CH_3)_2CHO^\bullet + H^+ \quad (11)$$

$$(CH_3)_2CHO^\bullet + {}^\bullet OH \rightarrow CH_3CHO + CH_3OH \quad (12)$$

Acetaldehyde was found in much lower quantity than propanone, both in the gas–solid and liquid–solid systems, indicating that reaction (12) represents a less significant side effect.

The presence of methanol was not confirmed in the reacting system probably because it was immediately decomposed to CO_2 or because its amount was too small to be determined.

It must be emphasized that both propanone and acetaldehyde were oxidized to CO_2 only in the gas–solid system, since only the species adsorbed on the catalyst surface were able to react.

On the contrary, in the liquid–solid system no CO_2 was detected, suggesting a relevant role played by a homogeneous attack of the hydroxyl radical. The presence of the sensitizer on the TiO_2 surface gave rise to an increase of the reaction rate, probably because the metal phthalocyanine could produce $^1O_2(\Delta)$ or $^\bullet O_2^-$ under irradiation [6,43–45].

4. Conclusions

The photocatalytic degradation of 2-PrOH occurred successfully in gas–solid and liquid–solid systems by using commercial TiO_2 both bare and impregnated with Sm, Gd and Ho double-decker phthalocyanine complexes. The sensitized samples were, in general, more photo-active than the bare TiO_2 for the 2-PrOH degradation, both in liquid–solid system and in gas–solid one although in the last conditions the increase of reactivity in the presence of the loaded samples was less significant. Moreover, the reactivity in the liquid–solid system was always higher than in the gas–solid one; it was about twofold for a 2-PrOH initial concentration of 915 pmm, whereas it was 5–6 times higher when the initial concentration of the substrate was 3660 ppm. This insight could be justified by the occurrence of a homogeneous reaction. Propanone and acetaldehyde were the main intermediates while carbon dioxide and water were the final oxidation products in the gas–solid system. No further oxidation of propanone and acetaldehyde to CO_2 was observed in the liquid–solid system.

Acknowledgements

The authors wish to thank Università degli Studi di Palermo for financial support (ex 60%).

References

[1] J.J. He, G. Benko, F. Korodi, T. Polivka, R. Lomoth, B. Akermark, L.C. Sun, A. Hagfeldt, V. Sundstorm, J. Am. Chem. Soc. 124 (2002) 4922.
[2] K. Ozoemena, N. Kuznetsova, T. Nyokong, J. Photochem. Photobiol. A.: Chem. 139 (2001) 217.
[3] K. Ozoemena, N. Kuznetsova, T. Nyokong, J. Mol. Catal. A: Chem. 176 (2001) 29.
[4] W. Spiller, H. Kliesch, D. Wöhrle, S. Hackbarth, B. Rodger, G. Schnurpfeil, J. Porphyrins Phthalocyanines 2 (1998) 145.
[5] G. Mele, G. Ciccarella, G. Vasapollo, E. García-López, L. Palmisano, M. Schiavello, Appl. Catal. B: Environ. 38 (2002) 309.
[6] G. Mele, R. Del Sole, G. Vasapollo, E. García-López, L. Palmisano, M. Schiavello, J. Catal. 217 (2003) 334.
[7] C.G. Clòaessens, W.J. Blau, M. Cook, M. Hanack, R.J.M. Nolte, T. Torres, D. Wöhrle, Monatsh. Chem. 132 (2001) 3 (and references therein).
[8] C.C. Leznoff, A.B.P. Lever, Phthalocyanines: Properties and Applications, vols. 1–4, VCH, New York, 1989–1996.
[9] J.W. Perry, K. Mansour, I.Y.S. Lee, X.L. Wu, P.V. Bedworth, C.T. Chen, D. Ng, S.R. Marder, P. Miles, T. Wada, M. Tian, H. Sasabe, Science 273 (1996) 1533.
[10] G. Guillaud, J. Simon, J.P. Germain, Coord. Chem. Rev. 178–180 (1998) 1433.
[11] N.B. McKeown, Phthalocyanine Materials: Synthesis, Structure and Function, Cambridge University Press, Cambridge, 1998.
[12] I.S. Kirin, P.N. Moskalev, Yu.A. Makashev, Zh. Neorg, Khim 12 (1967) 707.
[13] R. Słota, G. Dyrda, Inorg. Chem. 42 (2003) 5743.
[14] R. Słota, G. Dyrda, Z. Hnatejko, J. Karolczak, Z. Stryła, J. Porphyrins Phthalocyanines 10 (2006) 43.
[15] M. Schiavello (Ed.), Heterogeneous Photocatalysis, John Wiley & Sons, New York, 1995.
[16] N. Serpone, E. Pelizzetti (Eds.), Photocatalysis: Fundamentals and Applications, John Wiley & Sons, New York, 1989.
[17] A. Fujishima, K. Hashimoto, T. Watanabe, TiO_2 Photocatalysis: Fundamentals and Applications, Bkc, Tokyo, 1999.
[18] G. Mele, E. García-López, L. Palmisano, G. Dyrda, R. Slota, J. Phys. Chem. C 111 (2007) 6581.
[19] J. Peral, D. Ollis, J. Catal. 136 (1992) 554.
[20] R.I. Bickley, G. Munuera, F.S. Stone, J. Catal. 31 (1973) 398.
[21] S.A. Larson, J.A. Widengree, J. Falconer, J. Catal. 157 (1995) 611.
[22] F. Arsac, D. Bianchi, J.M. Chovelon, C. Ferronato, J.M. Herrmann, J. Phys. Chem. A 110 (2006), 4202 and 4213.
[23] B. Othani, K. Iwai, S. Nishimoto, S. Sato, J. Phys. Chem. B 101 (1997) 3349.
[24] A. Sclafani, J. Herrmann, J. Photochem. Photobiol. A: Chem. 113 (1998) 181.
[25] H. Yamashita, Y. Nishida, S. Yuan, K. Mori, M. Nirisawa, Y. Matsumura, T. Ohmichi, I. Takayama, Catal. Today 120 (2007) 163.
[26] D. Haffad, A. Chambellan, J.C. Lavalley, J. Mol. Catal. A: Chem. 168 (2001) 153.
[27] A. Gervassini, Y. Fenyvesi, A. Auroux, Catal. Lett. 43 (1997) 219.
[28] M.E. Manríquez, T. López, R. Gómez, J. Navarrete, J. Mol. Catal. A: Chem. 220 (2004) 229.
[29] E. Ortiz-Islas, T. López, J. Navarrete, X. Bokhimi, R. Gómez, J. Mol. Catal. A: Chem. 228 (2005) 345.
[30] S. Chavadej, P. Phuaphromyod, E. Gulari, P. Rangsunvigit, T. Sreethawong, Chem. Eng. J. 137 (2008) 489.
[31] A.B.P. Lever, Adv. Inorg. Radiochem. 7 (1965) 27.
[32] G. Martra, V. Augugliaro, S. Coluccia, E. García-López, V. Loddo, L. Marchese, L. Palmisano, M. Schiavello, Stud. Surf. Sci. Catal. 130 (2000) 665.
[33] M.C. De Rosa, R.J. Crutchley, Coord. Chem. Rev. 233 (2002) 351.
[34] C.S. Turchi, D. Ollis, J. Catal. 119 (1989) 483.
[35] C. Minero, G. Mariella, V. Maurino, E. Pelizzetti, Langmuir 16 (2000) 2632.

[36] G. Marcì, M. Addamo, V. Augugliaro, S. Coluccia, E. García-López, V. Loddo, G. Martra, L. Palmisano, M. Schiavello, J. Photochem. Photobiol. A: Chem. 160 (2003) 105.
[37] M. Addamo, V. Augugliaro, S. Coluccia, M. Faga, E. García-López, V. Loddo, G. Marcì, G. Martra, L. Palmisano, J. Catal. 235 (2005) 209.
[38] M. Addamo, V. Augugliaro, S. Coluccia, A. Di Paola, E. García-López, V. Loddo, G. Marcì, G. Martra, L. Palmisano, Int. J. Photoenergy 8 (2006) 1.
[39] W. Xu, D. Raftery, J.S. Francisco, J. Phys. Chem. 107 (2003) 4537.
[40] D. Carriazo, C. Martín, V. Rives, Catal. Today 126 (2007) 153.
[41] Y. Ohko, K. Hashimoto, A. Fujishima, J. Phys. Chem. A 101 (1997) 8057.
[42] H. Herrmann, S.T. Martin, M.R. Hoffmann, J. Phys. Chem. 99 (1995) 16641.
[43] R. Gerdes, D. Wöhrle, W. Spiller, J. Schneider, G. Schnurpfeil, G.S. Ekloff, J. Photochem, Photobiol. A: Chem. 111 (1997) 65.
[44] R. Bonnett, Chem. Soc. Rev. 24 (1995) 19.
[45] G. Mele, R. Del Sole, G. Vasapollo, G. Marcì, E. García-López, L. Palmisano, J. Coronado, M.D. Hernández-Alonso, C. Malitesta, M.R. Guascito, J. Phys. Chem. B 109 (2005) 12347.